Forecasting the inundation of postfire debris flows

Katherine R. Barnhart[1*], *Ryan P.* Jones[1], *David L.* George[2], *Francis K.* Rengers[1], and *Jason W.* Kean[1]

[1] U.S. Geological Survey, Box 25046 DFC MS 966; Denver, CO 80225, USA
[2] U.S. Geological Survey, 1300 SE Cardinal Court, Vancouver, WA 98683, USA

Abstract. In the semi-arid regions of the western United States, postfire debris flows are typically runoff generated. The U.S. Geological Survey has been studying the mechanisms of postfire debris-flow initiation for multiple decades to generate operational models for forecasting the timing, location, and magnitude of postfire debris flows. Here we discuss challenges and progress for extending operational capabilities to include modeling postfire debris-flow inundation extent. Analysis of volume and impacted area scaling relationships indicated that postfire debris flows do not conform to assumptions of geometric self-similarity. We documented sensitivity of impacted areas to rainfall intensity using a candidate methodology for generating inundation hazard assessments. Our results emphasize the importance of direct measurements of debris-flow volume, inundated area, and high temporal resolution rainfall intensity.

1 Introduction and history

Wildfire exacerbates debris-flow hazards by increasing surface-water runoff generation, erosion, and mobilization of sediment, and consequently, debris-flow sediment volumes. The role of fire in debris-flow initiation has been recognized in southern California, USA, for nearly a century [e.g., 1]. In contrast with debris flows generated from shallow landslides [2], postfire debris flows in the semi-arid western United States are typically initiated by overland flow scour, rainsplash, and rilling [3–5]. However, these initiation mechanisms are not unique to burned watersheds, and similar mechanisms can generate debris flows in unburned watersheds [6]. Burned watersheds may also be susceptible to shallow landslides [e.g., at times of partial hydrologic recovery, 7,8].

The U.S. Geological Survey (USGS) and the National Weather Service (NWS) have collaborated on postfire debris-flow early warning since 2005 [9]. Extensive monitoring of debris-flow-susceptible watersheds with high-temporal resolution rain gages and flow stage sensors [e.g., 10, and additional observational datasets cited in 11] yielded an understanding of what rainfall characteristics triggered postfire debris flows and an empirical model used to forecast the likelihood of a debris flow given a rainfall intensity [11,12]. The inputs to this empirical model include burn severity, 15-minute rainfall intensity (I_{15}), soil erodibility, and watershed topography. For calendar year 2021, 66 assessments totaling over 18,000 square kilometers were produced by the USGS. In addition to the empirical likelihood model, an empirical volume model was used for hazard assessments. The volume model assumes uniform rainfall over a watershed and was based on observations of debris-flow size, I_{15}, burn severity, and topographic characteristics [13]. The likelihood and volume models provided situational awareness about the timing and location of postfire debris flows, and the size of these flows (magnitude).

Existing capabilities do not provide information about the extent of debris-flow inundation, maps of which might provide situational awareness for land and emergency management professionals. Extending postfire debris-flow hazard assessments to include forecasts of runout requires the information used in current hazard assessments, and additional information such as identification of a suitable runout model, the ability to parameterize mobility characteristics, and the propagation of uncertainty in input constraints into uncertainty in impacted areas.

2 Scope

This study focuses on two questions central to widespread application of runout models. The two considered questions are not directly related; however, we considered them both because they highlight the challenges associated with two major aspects of forecasting postfire debris-flow runout: (1) understanding the relationship between mobility characteristics and parameterization of reduced complexity models, and (2) characterizing the sensitivity of inundation to rainfall intensity.

First, are the mobility characteristics of debris flows sourced in burned watersheds different from those originating from unburned watersheds? We took a simple approach to addressing this question and

* Corresponding author: krbarnhart@usgs.gov
Any use of trade, firm, or product names is for descriptive purposes only and does not imply endorsement by the U.S. Government. Elizabeth Singh-Search digitized runout from reference [1]. Comments from Marina Pirulli, Mark Reid, Dennis Staley, Rex Baum, Brian Shiro and Janet Carter improved the content and clarity of the manuscript.

compared the volume-inundated area scaling for debris flows from burned and unburned watersheds. Second, how does uncertainty in rainfall intensity used as input to the volume model [13] propagate into uncertainty in inundated area forecast by a runout model? We considered this question by testing an approach for generating a retrospective hazard assessment for the 9 January 2018 Montecito, California, USA, debris-flow event (hereafter "Montecito event") [14]. In this event, intense rain (I_{15}=84–99 mm/h) fell on the steep slopes of the Santa Ynez Mountains previously burned by the Thomas Fire, mobilizing sediment from hillslopes and channels [15,16] into multiple boulder-laden slurries that ran out onto a ~4 km-wide coalesced alluvial fan (Fig. 1) [14].

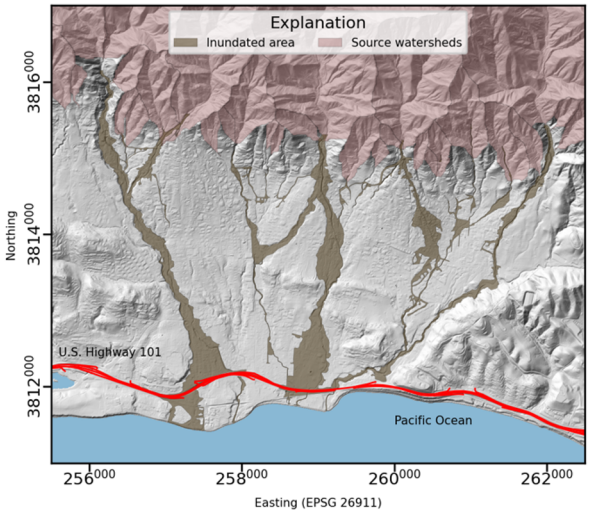

Fig. 1. Map of observed inundated area and potential source watersheds from the Montecito event.

3 Methods

3.1 Volume-area scaling

We evaluated the relationship between debris-flow volume, V, and inundated planimetric area, B for different mass flow types. We evaluated this relationship as a proxy for mobility characteristics. Previously, a relation between V and B was derived for lahars by postulating that lahars of diverse sizes were geometrically similar, implying a constant relationship between mean depth, $\bar{h}$, and B [17]: $\varepsilon = \bar{h}/\sqrt{B} = V/B^{3/2}$. These authors postulated that ε was a small constant. Conservation of mass results in $B = c\,V^{2/3}$ with $c = \varepsilon^{-2/3}$. Application of volume-area scaling relationships for estimation of inundation hazard zones requires that ε remains constant for different flows, an assumption confirmed for lahars, rock avalanches, and debris-flows [17,18].

We tested this assumption for runoff-generated debris flows from burned and unburned watersheds and compared the results with landslide-sourced debris flows and lahars. We compiled existing values of B and V for landslide-sourced debris flows and lahars [18,19], runoff-generated debris flows from burned watersheds [1,20–22], and debris flow events from the Italian Alps that were likely primarily runoff-generated but originated from unburned watersheds [23]. For each of the four mass flow types, we fit two linear statistical models relating $\log_{10}V$ and $\log_{10}\varepsilon$. The first model, M1, states that $\log_{10}\varepsilon$ can be described as a constant, a: $\log_{10}\varepsilon = a$, and the second model, M2, includes a dependence on the independent variable, $\log_{10}V$, using the coefficient b: $\log_{10}\varepsilon = a + b\log_{10}V$.

After fitting M1 and M2 with observations from each mass flow type, we compared the model fits using a standard Analysis of Variance (ANOVA) procedure, summarized by an F-statistic. The ANOVA tests the null hypothesis that none of the variation in the dependent variable, $\log_{10}\varepsilon$, is explained by the independent variable, $\log_{10}V$. A large value of the F-statistic indicates rejection of the null hypothesis that ε is not a constant.

We do not attempt to formally relate ε to debris-flow geotechnical properties or runout model mobility parameters. However, because ε relates mean depth and inundated area, it reflects flow mobility. An increase in ε at a given volume indicates a less mobile flow (a smaller extent or deeper deposit depth).

3.2 Uncertainty due to rainfall intensity

Prior work found that three different runout models were similarly successful at simulating the Montecito event [24], and simulation performance was more sensitive to debris-flow volume than debris-flow mobility. We built on this work and tested a simple candidate approach for generating a hazard assessment. For southern California, the link between rainfall and debris-flow volume is expressed with an empirical model developed by Gartner [13]. We coupled this empirical volume model with the D-Claw runout model [25,26] and considered four I_{15} value scenarios: 25, 50, 75, and 100 mm/h. For each watershed burned by the Thomas Fire and each I_{15} value, we calculated the sediment volume from the Gartner model and the water volume based on multiplying the watershed area with depth of rain associated with a 15-minute storm. Debris-flow material with sediment concentrations implied by the calculated water and sediment volumes was initialized using a triangular hydrograph following [27] at the watershed outlets delineated as part of the current likelihood and volume hazard assessment methodology. Following prior work [24], we used an initial permeability of k_0 = $1{\cdot}10^{-11}$ m^2, a critical state solid volume fraction of m_{crit} = 0.64, and a threshold of 0.3 m for minimum flow depth to depict debris-flow extent.

4 Results

4.1 Scaling analysis

We found that ε is not constant with volume for debris flows from burned watersheds (Fig. 2). Instead, ε has higher values for low volumes and decreases with increasing volume. This contrasts with lahars, which have a constant value of ε across the range of volume considered. The F-statistic for burned, runoff-generated debris flows was 37 (Table 1), consistent with rejecting the hypothesis that ε is constant. On the other hand, the

Table 1. Summary of linear model fits.

	Debris flows						Lahar (n=28)	
	Burned, runoff generated (n=62)		Unburned, landslide-sourced (n=50)		Unburned, runoff-generated (n=27)			
Model	M1	M2	M1	M2	M1	M2	M1	M2
Estimate *a*	-1.7***	0.12	-1.9***	-1.5***	-2.3***	-1.26**	-3.3***	-0.069***
Standard error *a*	0.11	0.32	0.073	0.21	0.099	0.52	0.087	0.070
Estimate *b*	NA	-0.49***	NA	-0.097*	NA	-0.24*	NA	-2.8
Standard error *b*	NA	0.08	NA	0.051	NA	0.12	NA	0.51
Residual standard error	0.86	0.69	0.49	0.48	0.48	0.45	0.46	0.46
Residual sum of squares	45	28	10	9.3	5.3	4.5	5.7	5.5
F-statistic (comparison to M1)	NA	37	NA	3.6	NA	3.9	NA	0.95
Probability(>F)	NA	$9.8 \cdot 10^{-8}$***	NA	0.062*	NA	0.061*	NA	0.34
Retain or reject null hypothesis that ε is constant	Reject		Retain at 90% confidence, reject at 95% confidence				Retain	

NA=not applicable. Stars denote confidence level *p<0.1; **p<0.05; ***p<0.01

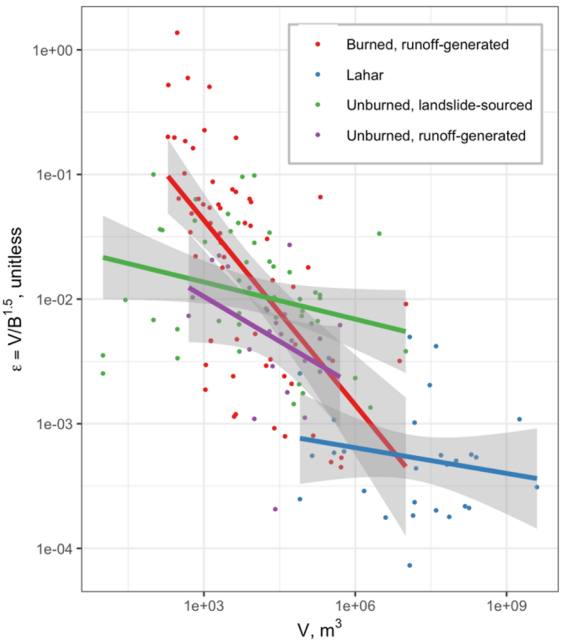

Fig. 2. Relation between deposit volume and ε for four mass flow types. Solid lines and gray region indicate M2 model fit and standard error, respectively.

F-statistic for the lahar category was 0.34, consistent with retaining the null hypothesis that ε is constant.

Debris flows sourced from shallow landslides and runoff generation in unburned watersheds showed a weak negative relation between ε and V (Fig. 2). The F-statistics for these two mass flow types were 3.6 and 3.9, respectively (Table 1), which resulted in retaining the null hypothesis that ε is constant at the 90% (p=0.1) confidence level or rejecting it at the 95% (p=0.05) confidence level.

The decrease in ε with increasing volume for debris flows from burned watersheds is consistent with a constant value of $\bar{h}$ across the more than four orders of magnitude for V in our compilation of observed events. For low values of V, ε for burned watersheds is larger than all other mass flow types. At high values of V, ε is comparable in magnitude to lahars. Rejection of the hypothesis that ε is constant implies that delineation of hazard zones using V-B scaling relationships cannot use a constant value for ε.

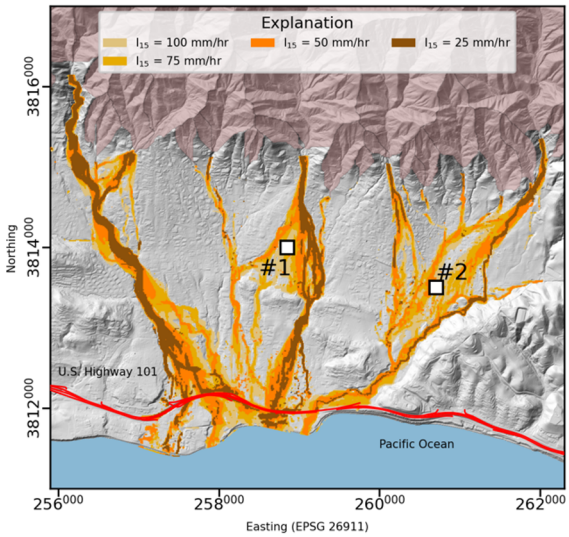

Fig. 3. Simulated inundation areas using different values of I_{15}. White boxes indicate locations discussed in the text.

4.2 Example forecast varying rainfall intensity

Simulations using different rainfall intensities resulted in substantially different inundation areas (Fig. 3). At I_{15} values of 25, 50, 75, and 100 mm/h, simulated inundation extents were 1.3, 2.6, 4.2, and 5.6 km^2, respectively. The I_{15} of 50 mm/h inundated a comparable total area as the observed event. The scenario with I_{15} of 100 mm/h inundated most but not all the area affected by the event and overpredicted inundation in some areas (square #1).

At the lowest I_{15} value, simulated debris-flow runout roughly followed the 5–20-m wide active channels that are most deeply entrenched within the coalesced alluvial fan. Most simulated flow paths were wider than this channel, reaching the lateral extent of the next most entrenched distributary channel. As the I_{15} increased, the

extent of inundation increased, and included areas unconfined by a channel at any scale. The areas with the largest mismatch between model and observation were those where topography does not confine the flow (square #2)

5 Discussion

Our results indicate that geometric self-similarity does not hold for debris flows generated by burned watersheds. This finding implies that reduced complexity models that rely on volume-area scaling relationships to determine the distal extent of affected areas based on volume cannot adequately represent postfire hazard assessment using a single value of ε. We considered that this result may have occurred because most postfire debris flows are runoff-generated rather than sourced from discrete slope failures. For example, runoff-generated debris flows may have a lower solid volume fraction than slope failure-sourced debris flows. However, this explanation is not consistent with the analysis of data from the Italian Alps [23], where debris flows originate from runoff process, indicating a constant value of ε (at the 90% confidence level). The contrast may indicate a process difference in the inundation dynamics of runoff generated debris flows from burned and unburned watersheds.

The example forecast at Montecito, California, (Fig. 3) demonstrates the strong sensitivity that I_{15} has on affected area. Specifically, because inundated area increased with increasing rainfall intensity, accurate forecasting benefits from input of a range of plausible intensities. This sensitivity originates from the importance of I_{15} in the empirical volume model [13]. Development of postfire debris-flow inundation hazard assessments for areas outside of southern California would warrant either validation of the southern California volume model or the establishment of new, location-specific volume models. An alternative is the generation of physical process-based volume models. Creation of empirical volume models involves direct observation of mobilized volume and candidate independent variables, specifically high-temporal-resolution rainfall.

6 Outlook and conclusions

Forecasting postfire debris-flow runout is feasible because of extensive work documenting the mechanisms, timing, susceptibility, and magnitude of this this type of debris flow. Generation of a reliable methodology for runout hazard assessments would benefit from more detailed case studies that document initiation mechanisms, high temporal-resolution rainfall, total mobilized volume, deposit extent, and geotechnical properties of hillslope materials and debris-flow slurries. Two potential research areas are (1) generating new or validating existing capabilities for event volumes outside of southern California; and (2) linking field observations, laboratory geotechnical measurements, and model parameters describing debris-flow mobility.

References

1. W.D. Chawner, *The Montrose-La Crescenta (California) Flood of January 1, 1934, and Its Sedimentary Aspects*, MS Thesis, California Institute of Technology (1934)
2. R.M. Iverson, Rev. Geophys. **35**, 245 (1997)
3. S.H. Cannon, R.M. Kirkham, and M. Parise, Geomorphology **39**, 171 (2001)
4. S. H. Cannon, J. E. Gartner, R. C. Wilson, J. C. Bowers, et al., Geomorphology **96**, 250 (2008)
5. K.M. Schmidt, M.N. Hanshaw, J.F. Howle, J.W. Kean, et al., Ital. J. Eng. Geol. Environ. 583 (2011)
6. J.A. Coe, D.A. Kinner, and J.W. Godt, Geomorphology **96**, 270 (2008)
7. F.K. Rengers, L.A. McGuire, N.S. Oakley, J.W. Kean, et al., Landslides **17**, 2631 (2020)
8. M.A. Thomas, F.K. Rengers, J.W. Kean, L.A. McGuire, et al., J. Geophys. Res. Earth Surf. **126**, e2021JF006091 (2021)
9. NOAA-USGS Debris Flow Task Force, *NOAA-USGS Debris-Flow Warning System—Final Report* (2005)
10. J.W. Kean, D.M. Staley, and S.H. Cannon, J. Geophys. Res. **116**, F04019 (2011)
11. D.M. Staley, J.A. Negri, J.W. Kean, J.L. Laber, et al., Geomorphology **278**, 149 (2017)
12. S.H. Cannon, J.E. Gartner, M.G. Rupert, J.A. Michael, et al., GSA Bull. **122**, 127 (2010)
13. J.E. Gartner, S.H. Cannon, and P.M. Santi, Eng. Geol. **176**, 45 (2014)
14. J.W. Kean, D.M. Staley, J.T. Lancaster, F.K. Rengers, et al., Geosphere **15**, 1140 (2019)
15. P. Alessio, T. Dunne, and K. Morell, J. Geophys. Res. Earth Surf. **126**, e2021JF006108 (2021)
16. K. Morell, P. Alessio, T. Dunne, and E. Keller, Geophys. Res. Lett. **48**, e2021GL095549 (2021)
17. R.M. Iverson, S.P. Schilling, and J.W. Vallance, Geol. Soc. Am. Bull. 13 (1998)
18. J.P. Griswold and R.M. Iverson, *Mobility Statistics and Automated Hazard Mapping for Debris Flows and Rock Avalanches* (2008)
19. C.S. Magirl, P.G. Griffiths, and R.H. Webb, Geomorphology **119**, 111 (2010)
20. S.H. Cannon, P.S. Powers, R.A. Pihl, and W.P. Rogers, *Preliminary Evaluation of the Fire-Related Debris Flows on Storm King Mountain, Glenwood Springs, Colorado* (1995)
21. D. Bernard, E. Trousil, and P. Santi, Eng. Geol. **285**, 105991 (2021)
22. S. Wall, *Predictive Models of Post-Wildfire Debris Flow Volume and Grain Size Distribution in the Intermountain West*, MS Thesis, Utah State University (2021)
23. M. Berti and A. Simoni, Geomorphology **90**, 144 (2007)
24. K.R. Barnhart, R.P. Jones, D. L. George, B.W. McArdell, et al., Geophys. Res. Earth Surf. **126**, e2021JF006245 (2021)
25. D.L. George and R.M. Iverson, Proc. R. Soc. Math. Phys. Eng. Sci. **470**, 20130820 (2014)
26. R.M. Iverson and D.L. George, Proc. R. Soc. Math. Phys. Eng. Sci. **470**, 20130819 (2014)
27. D. Rickenmann, Nat. Hazards **19**, 47 (1999)